Extending the Objective Motion Cueing Test to Measure Rotorcraft Simulator Motion Characteristics

Dalmeijer, W.; MiletoviC, Ivan; Stroosma, Olaf; Pavel, M. D.

Publication date
2017

Document Version
Accepted author manuscript

Published in
73rd Annual AHS International Forum and Technology Display

Extending the Objective Motion Cueing Test to Measure Rotorcraft Simulator Motion Characteristics

Wouter Dalmeijer
MSc Student
Delft University of Technology
Delft, Netherlands

Ivan Miletović
PhD Student
Delft University of Technology
Delft, Netherlands

Olaf Stroosma
Researcher
Delft University of Technology
Delft, Netherlands

Marilena Pavel
Assistant Professor
Delft University of Technology
Delft, Netherlands

ABSTRACT

In search of a more objective way to evaluate motion cueing fidelity, the Objective Motion Cueing Test (OMCT) was proposed by Advani and Hosman in 2006. However, an application of this test for rotorcraft has not yet been studied. The objectives of this paper are therefore (1) to investigate the extent to which the OMCT is representative for rotorcraft, (2) to investigate whether a potentially superior OMCT, better representing helicopter motion, can be defined and (3) to validate potential differences in the prediction of motion characteristics between an OMCT based on the helicopter motion, and the current OMCT, with a pilot-in-the-loop experiment on the SIMONA Research Simulator (SRS). It was found that the current OMCT has a set of input signals which is representative for helicopter heave motion, but might not be representative for pitch and surge motion characteristics. Using an OMCT tailored to longitudinal helicopter motion, notable differences in helicopter pitch and surge motion characteristics were found. Using pilot-in-the-loop simulation data, the effect of pilot control behaviour on the proposed methodology was studied. It was seen that, although differences were identified, the main trend of the frequency response functions was determined by the dynamics of the helicopter model. It is recommended to evaluate the current set of input signals of the OMCT for a variety of models, also incorporating lateral motion, and tasks using a similar method presented in this article.

INTRODUCTION

For simulator certification, the integrated performance of motion cueing systems is evaluated using subjective pilot assessment, according to ICAO guidelines in Ref. 1. This means that before a simulator can be used for training, an experienced test pilot evaluates its performance. Based on his feedback, engineers then modify the settings of the Motion Cueing Algorithm (MCA). A disadvantage of subjective assessment however, is that the results are often hard to repeat, that is, different pilots may assess the same motion cueing system differently, as was stated in Ref. 2.

In search for a method to more objectively evaluate simulator performance the Objective Motion Cueing Test (OMCT) was proposed by Advani and Hosman in Ref. 3 in 2006. Similarly to Sinacori in Ref. 4, the OMCT studies the gain and phase shift of the MCA. However, whereas Sinacori only studies the frequency response at 1 $[rad/s]$, the OMCT evaluates cueing performance by constructing so-called frequency response functions of the motion system, by exciting the motion system with a sinusoidal input signal at 12 predefined frequencies. Each of the six axes is excited separately, resulting in six direct frequency response functions. Furthermore, to study inter-axes coupling, four extra tests are included to study pitch-surge and roll-sway coupling. Table 1 gives a matrix containing the input and output axes for longitudinal tests. The OMCT was added as an amendment to ICAO document 9625 in Ref. 1 in 2009.

Table 1: Longitudinal OMCT test numbers, according to Ref. 3.

Input Axis	Output Axis		
	Pitch	Surge	Heave
Pitch	1	2	-
Surge	7	6	-
Heave	-	-	10

An effort has been made to combine the OMCT with a criterium for motion fidelity. A criterium for motion fidelity was proposed by Advani and Hosman in 2007, given in Ref. 5, but was not adopted. In 2013, a practice of industries best standards was given by Hosman in Ref. 6 and again in 2016 in Ref. 7. At this point, a fidelity criterium does not exist. the OMCT is therefore a useful tool to investigate motion characteristics of different cueing settings, but unfortunately not

(yet) a stand-alone method to evaluate the motion fidelity.

Practical implementation of the OMCT was described in Ref. 8 in 2013. On the limitations of the OMCT, Stroosma concludes that due to uncoupled input axes and assumed linearity of the input spectrum the OMCT may give an incomplete picture of motion characteristics:
"Input signals may have abstracted away some characteristics of the aircraft motions that play an important role in operational use. An example is the fact that for large [fixed-wing] aircraft a yaw motion is usually also accompanied by a sway specific force due to the distance of the pilot station to the center of gravity." Ref. 8

In the time domain, these abstractions become apparent. Figure 1 shows the motion output of a helicopter model during 10 $[s]$ of hover in a longitudinal pilot-in-the-loop simulation, together with the input signal of an OMCT for a pitch frequency response function. For this particular test, the OMCT excites the MCA with $A_i sin\omega_i t$ on the pitch rotational channel. However, since it is assumed that aircraft pitch-surge motion is uncoordinated, also a term $gsin\theta$ is put on the surge channel. In this case, θ is the aircraft pitch angle. Heave motion is not excited.

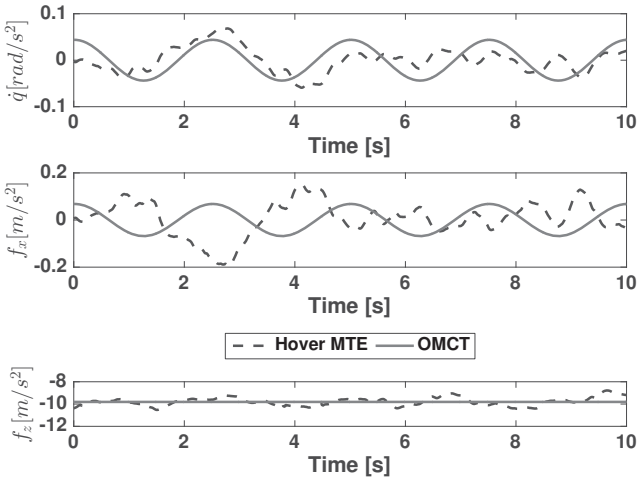

Fig. 1: Typical motion input to the MCA for a helicopter during hover, plotted together with the seventh input signal for the pitch frequency response function, OMCT test 1, ($\omega_7 = 1.585[rad/s]$).

It can firstly be seen that the OMCT excites only pitch and surge axes, whereas during a hover simulation all three longitudinal degrees-of-freedom are excited. Secondly it can be seen that the OMCT input signals are not of the same phase as those of the hover task. Looking at the specific force in surge direction, f_x, from 1 to 5 $[s]$, it can be seen that the OMCT excites this axis at roughly 180 $[deg]$ phase difference with the helicopter motion, whereas at the same time the pitch axis, $\dot{q}$, is excited with a similar phase, 0 $[deg]$.

Furthermore, Seehof concluded in 2014 the following on general applicability of the OMCT for all aircraft and training purposes in Ref. 9:

- The OMCT uses a simplified set of input signals. For example, during take-off, in surge direction, the accelerations of the aircraft might be larger than 1 $[m/s^2]$, which is the amplitude prescribed by the OMCT. Results of the OMCT therefore may not be representative for this particular maneuver.
- The training purpose of the simulation may vary to a large extent. Up to now, no helicopter simulation has been investigated with respect to the OMCT.

For a representative test in the case of figure 1, the addition of all 12 OMCT input signals should result in a signal with similar characteristics as the hover task of figure 1. However it can be seen that the amplitude of for example the surge input is similar to that of the hover task, already for just one frequency. A reconstruction of all 12 frequencies would likely result in a signal with too large amplitude for this task.

From previous research it can be thus be concluded that doubts exist about the extent to which the OMCT is representative in the helicopter domain. Underlying assumptions of the OMCT about the motion of fixed-wing aircraft may not be fully transferable. The first objective of this paper is therefore to investigate the extent to which the OMCT is representative for rotorcraft. A second objective is to investigate whether a potentially superior set of input signals better representing helicopter motion can be defined. A third objective is to validate potential differences in the prediction of motion characteristics between an OMCT based on the helicopter motion and the current OMCT with a pilot-in-the-loop experiment on the SIMONA Research Simulator (SRS).

EFFECT OF OMCT ASSUMPTIONS ON THE FREQUENCY RESPONSE FUNCTIONS

From literature two main assumptions of OMCT input signals on helicopter motion were identified: an uncoupled input and a linearity of the input spectra. However, what is the influence of these assumptions on the evaluation of motion characteristic of a classical washout algorithm in the longitudinal plane?

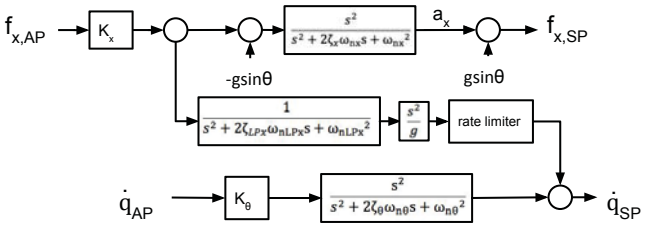

Fig. 2: Schematic representation of a cueing algorithm for pitch and surge in the longitudinal plane.

Figure 2 shows a schematic representation of a classical washout algorithm based on Reid an Nahon, Ref. 10, but for pitch acceleration and surge acceleration only. In figure 2, surge and pitch acceleration from the mathematical model are indicated with indices *AP* and the outgoing motion to

the simulator is indicated with indices *SP*. Two main channels can be distinguished: a translational channel and a rotational channel. Furthermore, sustained accelerations are simulated by means of tilt coordination channel. Figure 3 shows a schematic representation of a classical washout algorithm for heave.

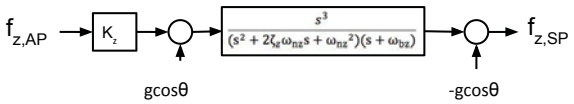

Fig. 3: Schematic representation of a cueing algorithm for heave in the longitudinal plane.

Note that all frequency response functions presented in this paper were obtained using a classical washout algorithm according to figure 2 and figure 3. Parameters were set according to table 2, unless specifically specified otherwise.

Table 2: Longitudinal settings for the classical washout algorithm.

	K $[-]$	ω_n $[rad/s]$	ζ $[-]$	ω_b $[rad/s]$	ω_{LP} $[rad/s]$
Pitch	0.7	0.8	1.0	0.0	-
Surge	0.7	1.0	1.0	0.0	2.0
Heave	0.5	2.5	1.0	0.2	-

Coupling of Input Signals

Crosstalk from Surge to Pitch The most important coupling in the cueing algorithm is crosstalk from surge to pitch. Sustained surge motion is simulated by tilting the simulator through a low-pass filter in the tilt coordination channel. This form of crosstalk is studied by the OMCT in 2 tests. Firstly in test 7 the surge axis is excited and the output on the pitch axis is measured, resulting in a pitch frequency response function due to an input on surge. Figure 4 shows the gain, $|H_7|$, and phase, $\angle H_7$ of test 7 for different cueing settings.

It should be noted that the simulator pitch angle was taken as output for this test, as was done by Hosman in Ref. 7, as opposed to the simulator pitch acceleration, as was done by Stroosma in Ref. 8. Since test 7 is essentially a frequency response function of the low-pass filter in the tilt coordination channel, such a representation can be more intuitively related to the MCA.

A typical tuning purpose of this test would be to determine the low-pass break frequency of the tilt coordination channel. As can be seen from figure 4, a higher break frequency will result in more cross coupling from surge to pitch, since the gain is larger for higher break frequencies. However, it is hard tune the algorithm based on this figure alone. It is is not clear which combination of gain and phase results in a simulation with a high predicted motion fidelity. Crosstalk from surge to pitch is a false cue, but due to the presence of tilt coordination

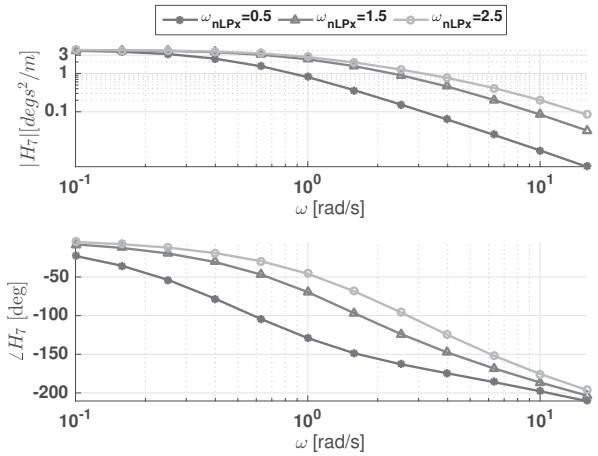

Fig. 4: Pitch frequency response function for a surge input, test 7 of the OMCT.

unavoidable. The gain of test 7 should not be as low as possible. However, a too large gain might result in unwanted pitch acceleration.

A solution to this problem might be to compare the results from test 7 with vestibular thresholds, such as obtained in Ref. 11. The hypothesis here is that if the frequency response function stays below thresholds of the semi-circular canals, the crosstalk from surge to pitch is acceptable. However, it could be that the characteristics of the crosstalk are sub-threshold in the frequency-domain, but are super-threshold in the time domain. Secondly motion cues presented to the pilot do not only depend on the cueing system, but also on the motion of the aircraft, which is not taken into account with such an approach. Another way to get a more complete picture of the pitch motion characteristics is to combine test 7 with a direct pitch frequency response function, test 1.

Test 1 studies crosstalk from surge to pitch in a pitch frequency response function using both surge and pitch input. Since for fixed-wing aircraft it is assumed that there is an uncoordinated motion between pitch and surge, also a signal is fed into the simulator on surge: $f_x = gsin(\theta)$. These signals were visualized in the time domain in figure 1. The frequency-domain response is visualized in figure 5.

In figure 5 three situations are depicted. Firstly a frequency response function from the current OMCT is depicted, indicated by $f_x = gsin(\theta)$. Helicopter motion is mostly coordinated, which is a common assumption for helicopter dynamics in simulator fidelity research, used for example in Ref. 12 and Ref. 13. This is an indication that during a regular helicopter task, $f_x = \dot{u} - gsin(\theta) \cong 0$. In figure 5 this scenario is represented by $f_x = 0$. Thirdly a test is shown were instead of $f_x = gsin(\theta)$, $f_x = -gsin(\theta)$ is cued. This is corresponding to the findings from figure 1, where it was seen that the relative phase difference between pitch and surge was roughly 180 $[deg]$ between 1 and 5 $[s]$.

It can be seen that the choice of input on the surge channel significantly influences pitch motion characteristics, especially at low frequencies.

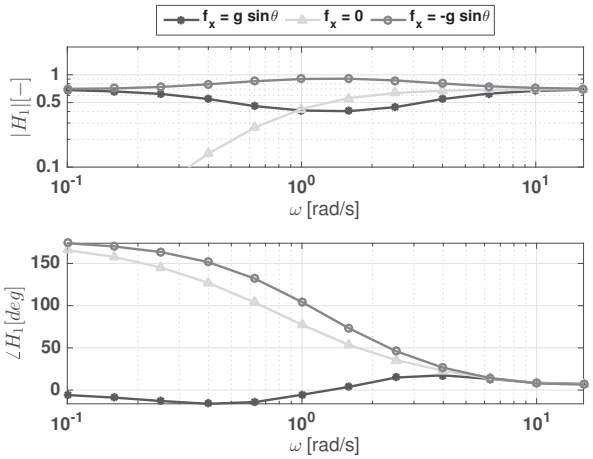

Fig. 5: Pitch frequency response computed with an input on pitch and surge axes, test 1 of the OMCT

Crosstalk from Pitch to Surge Crosstalk from pitch to surge originates from the transformation between the aircraft body frame of reference and the simulator inertial frame, indicated by $-gsin\theta$ in figure 3 and the transformation from the inertial frame of reference of the simulator to the simulator body frame, indicated by $gsin\theta$. θ in this case is the filtered pitch angle of the simulator. The OMCT studies this crosstalk by means of test number 2. Figure 6 shows a surge frequency response function due to an input on the pitch and surge channels.

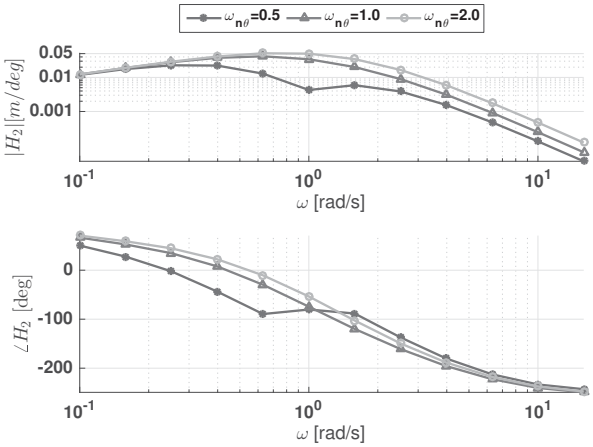

Fig. 6: Surge frequency response function due to pitch input, test 2 of the OMCT.

A typical tuning purpose of this test would be to determine the high-pass break frequency of the pitch channel. As can be seen from figure 6, a higher break frequency will result in more cross coupling from pitch to surge. However, as was the case for figure 4, the results from figure 6 are hard to interpret.

- As for test 1 displayed in figure 5, both an input on pitch axis and on the surge axis is used for this test. Therefore, not only is pitch-surge coupling included, but also surge-pitch coupling.
- Furthermore, surge acceleration a_x, not specific force f_x is taken as the output for this test.
- Cross talk from pitch to surge is a false cue but, like surge-pitch crosstalk not entirely unavoidable, as was discussed in Ref. 12. Similar to figure 4, it is therefore hard to judge surge motion characteristics based on test 2 alone. For a more complete picture of surge motion fidelity, test 2 should therefore be combined with a direct surge frequency response function, test 6 of the OMCT.

Linearity of Input Signals

From figure 1, it was seen that the amplitude of the surge input for an OMCT for pitch motion characteristics is larger than the actual input on the surge axis during pilot-in-the-loop hover simulation. The difference in amplitude might affect the OMCT for all non-linear elements in the motion cueing algorithm. Looking at figure 2 and figure 3, it can be seen that the most important non-linear element in the filter is the rate limiter in the tilt coordination channel. This limiter is present in the MCA to ensure that rotational rates from the tilt coordination channel are below perception thresholds. OMCT sensitivity to rate limiting was studied by Advani and Hosman in Ref. 7.

The effect of this non-linearity is illustrated by looking at test 6 with different amplitudes of the input spectrum, given in figure 7.

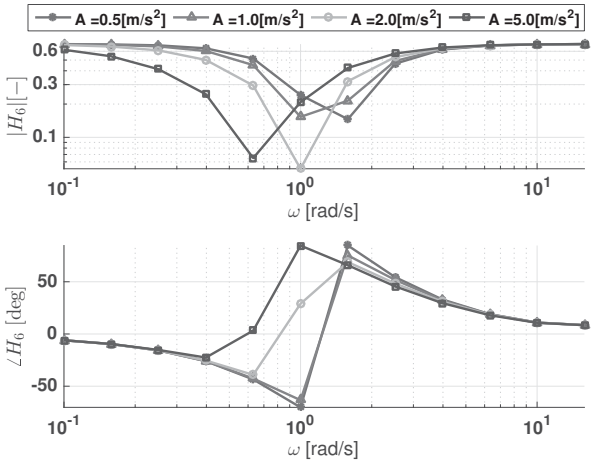

Fig. 7: Surge frequency response function computed using an input signal on the surge axis, $f_x = Asin(\omega t)$, with different amplitudes, test 6 of the OMCT.

It can be seen that for this particular motion setting, the frequency response at the Sinacori frequency of 1 $[rad/s]$ ranges from a modulus from 0.05 to 0.3. In practice this means that this cueing setting can have an OMCT gain varying with a factor 6 depending on the method of evaluation.

Issues with a possible implementation of the OMCT in the helicopter domain can be summarized essentially in three categories. Firstly surge-pitch coupling is represented incorrectly in the direct pitch frequency response function, figure 5. Secondly the results from cross coupling tests 2 and 7, given by

figure 6 and figure 4 respectively, are hard to interpret. Finally there is a large sensitivity to rate limiting in the tilt coordination channel.

These issues boil down to to the fact that the OMCT might not incorporate knowledge about the physical motion of the helicopter sufficiently. Therefore, to find a more representative set of input signals for the OMCT, helicopter motion in the longitudinal plane needs to be studied in the frequency domain.

A BETTER OMCT?

An off-line simulation using a helicopter model and a non-human controller was conducted. Time traces of this simulation were thereafter transformed to the frequency domain and used to tailor a set of input signals, and subsequently an OMCT, to the motion of the off-line simulation.

Setting Up an Off-line Simulation

A reference task is needed for the set-up, yielding a reference trajectory that is representative for regular helicopter simulator training operations. Secondly it should be standardized, such that any results from this analysis can be compared to other research. A third requirement would be that the trajectory should sufficiently excite the dynamics of the aircraft on the frequency range of the OMCT.

Considering these requirements it was decided to use a Mission Task Element (MTE) from ADS-33, Ref. 14, a military design standard for handling qualities requirements. The resulting off-line simulation is schematically represented in figure 8.

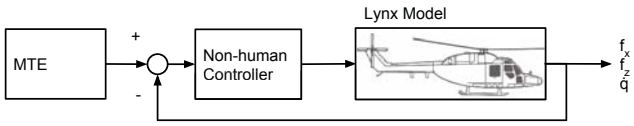

Fig. 8: Schematic flow chart of the off-line simulation.

A longitudinal MTE which is frequently used in simulator training, is an aborted take-off, referred to from now on as a take-off and abort. This task is initiated during hover at 35 $[ft]$ wheel height. The helicopter is accelerated to 40-50 $[kts]$, keeping the altitude constant as much as possible, at which point the take-off is aborted and the helicopter is decelerated back to hover again. Figure 9 shows the velocity profile of the take-off and abort MTE.

The goal of this MTE is to perform the maneuver in as little time as possible. The maneuver should be stopped if the helicopter is stabilized in hover at 800 [ft] from the starting point of the task. Figure 3 gives the desired and adequate performance for this task.

As can be seen from figure 9, the take-off and abort task is maneuver containing mainly low-frequency signals. To excite the higher frequencies on the OMCT spectrum, it was

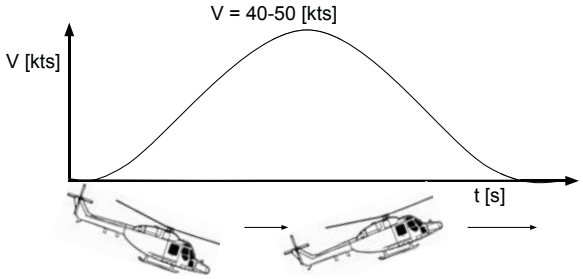

Fig. 9: Schematic of the Take-Off and Abort Mission Task Element.

Table 3: Adequate and desired longitudinal performance for a take-off and abort Mission Task Element.

	Adequate	Desired
Altitude $[ft]$	< 75	< 50
Time to complete $[s]$	< 30	< 25

therefore decided to also study a hover MTE using turbulence, since this task is more precise and requires higher frequency inputs from the controller.

A hover MTE is started at a small forward velocity of 6-10 $[kts]$. It is the goal of the pilot to stabilize the helicopter in hover at a specific location and remain in stabilized hover for 30 $[s]$. Figure 10 shows the velocity profile of a hover MTE.

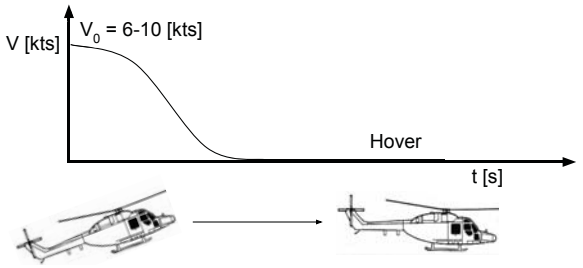

Fig. 10: Schematic of the Hover Mission Task Element.

Figure 3 gives the desired and adequate performance for this task.

To control the aircraft during these two MTEs, a controller consisting of two parts was designed and implemented. Firstly there is a PD controller, controlling the collective to keep the altitude constant throughout the maneuver. Secondly there is a PID controller computing a desired cyclic pitch to follow a velocity trajectory, according to the specific Mission Task Element.

A 3 Degrees-Of-Freedom, non-linear, longitudinal helicopter model was implemented, with numerical values taken from a DRA Research Lynx, Ref. 15. Equations of motion are given in appendix A. The following assumptions made on the dynamics and on the main rotor blades have particular influence on a tailored set of OMCT input signals.

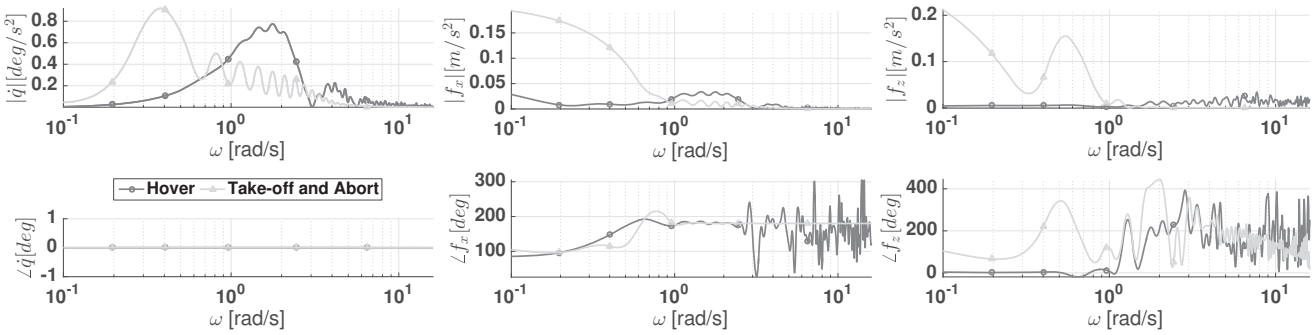

(a) Pitch. **(b) Surge.** **(c) Heave.**

Fig. 11: Amplitude and relative phase spectra used for a tailored OMCT.

Table 4: Adequate and desired longitudinal performance for a hover Mission Task Element.

	Adequate	Desired
Time to stabilize $[s]$	< 8	< 3
Longitudinal position $[ft]$	$+/-6$	$+/-3$
Altitude$[ft]$	$+/-2$	$+/-5$

- Fuselage drag was estimated by $D = C_D \frac{1}{2} \rho V^2 S$, with $C_D = 0.08[-]$ taken from Ref. 15. All other aerodynamic forces on the fuselage were neglected.
- A non-eccentric, spring-less flapping hinge and no drag forces on the main rotor were assumed. The effect of this assumption is that there are no moments or drag acting on the main rotor hub. Since these forces are small compared to the thrust force, as was stated in Ref. 16, this is considered a valid assumption for the purposes of this research.
- Quasi-steady inflow velocity and flapping dynamics are assumed.
- The engine is assumed to deliver the power required without delay, resulting in a constant RPM.

The result of these assumptions is that the only contributions to the specific forces in surge and heave direction are the main rotor thrust and the fuselage drag force. Furthermore, any pitch rotational acceleration is due to the main rotor thrust force.

To excite the higher frequencies on the OMCT spectrum, a turbulence model was implemented during the hover MTE. This turbulence model set a deviation from the body velocities u and w are using a Dryden spectrum according to Ref. 17. No rotational component in the turbulence was used.

Time traces of specific forces f_x and f_z and pitch acceleration $\dot{q}$ were computed for both MTEs. These time traces were subsequently converted to the frequency domain by means of the Fast Fourier Transform (FFT). This process results in 2 sets of 3 Power Spectral Densities (PSDs).

Tailoring the Input Signals

The amplitude from the PSDs can be used to make an estimate of a tailored amplitude spectrum directly. However, it is of importance to capture the relative phase between degrees of freedom. From figure 5 it was seen for example, that an OMCT pitch frequency response function is influenced significantly by the input of the surge axis. If the surge axis is excited by $gsin\theta$, the pitch motion characteristics at lower frequencies seem favourable. However, if the surge axis is excited by an input with 180 $[deg]$ relative phase difference, or $-gsin\theta$, there is a 180 $[deg]$ phase shift in the response function at low frequencies.

Following this reasoning it was decided to use both the amplitude and *phase* information from the PSDs. The absolute phase of the pitch axis was therefore set to zero and the *relative* phase for surge and heave was computed according to:

$$\angle f_x = \angle \dot{q} - \angle f_x \tag{1a}$$
$$\angle f_z = \angle \dot{q} - \angle f_z \tag{1b}$$
$$\angle \dot{q} = 0 \tag{1c}$$

However, due to the characteristics of the FFT, not on every OMCT frequency there is an estimate of the amplitude and phase. Therefore a model was made based on univariate splines to estimate amplitude and phase on OMCT frequencies. One set of input signals for the take-off and abort task and one set for the hover MTE were determined. Figure 11 shows the amplitude and relative phase models for pitch-surge and heave respectively.

Several interesting observations can be made from figure 11.

- Firstly it can be seen that amplitude at most points is a factor 50 times smaller than 1 $[m/s^2]$, which is the amplitude used for the current OMCT according to Ref. 1. This indicates that the signals going into the classical washout algorithm are over-sized in the original OMCT for this specific MTE and helicopter model.

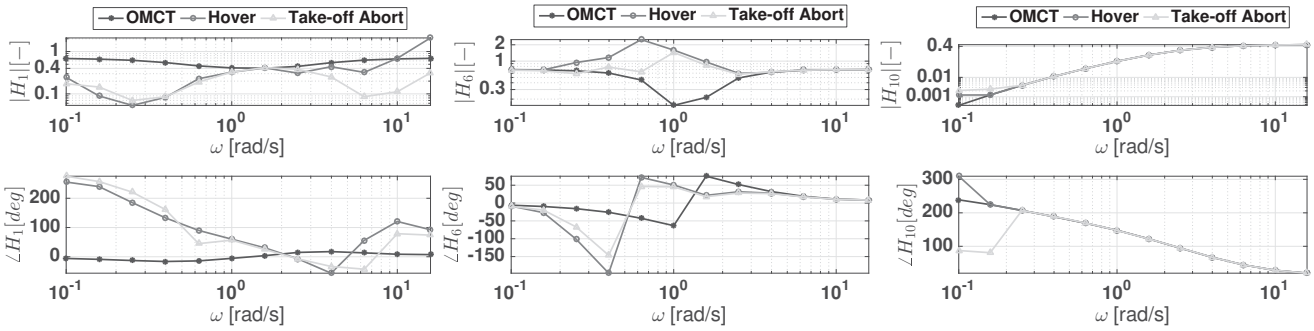

(a) Pitch. **(b) Surge.** **(c) Heave.**

Fig. 12: Comparison between two tailored OMCTs and the original OMCT.

- Secondly it can be seen that noise is present in the signals for frequencies above 2 $[rad/s]$. This noise due to a combination of the effect of atmospheric turbulence for the hover task and windowing from the FFT.
- Thirdly, the relative phase in figure 11b shows that the relative phase between pitch and surge is about 100 $[deg]$ for low frequencies and about 180 $[deg]$ for $\omega > 0.7[rad/s]$. A positive pitch motion therefore means a negative surge acceleration and vice versa.

A mathematical explanation for the last observation can be sought in the equations of motions that were used for the helicopter model. The expression for the specific force in surge direction is given by:

$$f_x = -\frac{D}{m}\cos\theta_f - \frac{T}{m}\sin(\theta_{1c} - \alpha_1) \tag{2}$$

In this expression, θ_f is the pitch angle of the helicopter, θ_{1c} is the angle of the control plane and α_1 is the longitudinal flapping angle. However, since pitch acceleration is solely caused by the thrust force, the second term in equation 2 can be substituted, resulting in the following expression,

$$f_x = -\frac{D}{m}\cos\theta_f - \frac{I_{yy}}{mh_R}\dot{q} \tag{3}$$

where I_{yy} is the moment of inertia of the helicopter body and h_R is the distance between the c.g. and the rotor hub.

To evaluate the relative phase between f_x and $\dot{q}$, it is important to note that angular acceleration is the double derivative of the helicopter pitch angle, $\dot{q} = \ddot{\theta}_f$. If it is assumed that $q \doteq \sin(\omega t)$ then $\theta_f = -\frac{1}{\omega^2}\sin(\omega t) = -\frac{1}{\omega^2}\dot{q}$. Substituted into equation 3 this gives:

$$f_x = -\frac{D}{m}\cos(-\frac{1}{\omega^2}\dot{q}) - \frac{I_{yy}}{mh_R}\dot{q} \tag{4}$$

It can be seen that for high frequencies, $-\frac{1}{\omega^2}\dot{q}$ becomes small, and f_x is only influenced by $-\frac{I_{yy}}{mh_R}\dot{q}$, meaning that the relative phase between pitch and surge for high frequencies is that of $-\frac{I_{yy}}{mh_R}$ or 180 $[deg]$.

Tailoring the OMCT

During pilot-in-the-loop simulation, different DOFs are excited simultaneously. Therefore it was decided to use the tailored input signals to excite different DOFs *simultaneously*.

A classical washout algorithm as was given in figure 2 and figure 3 with a parameter set equal to that of table 2 was excited on pitch, surge and heave *simultaneously*. The result is presented in figure 12, where the tailored OMCT is compared to the original OMCT. Figure 12a, figure 12b and figure 12c show the frequency response functions of the pitch channel, the surge channel and the heave channel respectively.

It was chosen to tailor the OMCT using the same 12 prescribed OMCT frequencies ranging from 0.1 to 15.8 $[rad/s]$, since a larger amount of frequencies would hinder any practical implementation of a tailored test in the future. Since all axes are excited simultaneously, the cross tests for the original OCMT lose their significance and are no longer performed.

The following observations can be made from the comparison between the original and tailored OMCT.

- At low frequencies for the pitch frequency response function, the current OMCT predicts favorable motion characteristics, with a gain of close to 1 and a phase close to 0 $[deg]$. However, both the tailored OMCT based on the hover task and on the take-off and abort task predict poor motion characteristics with a low gain and a phase around 200 $[deg]$ lead. This is an indication pitch-surge motion in this case is more coordinated, corresponding to the case of $f_x = 0$ in figure 5. At high frequencies upswing is present in the hover task. For the take-off and abort task, the gain is lower than the current OMCT. These phenomena are the result of crosstalk from the surge to the pitch axis. Similarly to figure 4, in figure 13 the low-pass break frequency on the tilt coordination channel was varied.
  From figure 13 it can be seen that when tuned such that little coupling is expected from surge to pitch, the pitch frequency response function resembles a high-pass filter.
- From figure 12b it can be seen that the surge frequency response function for the original OMCT predicts a 'gap'

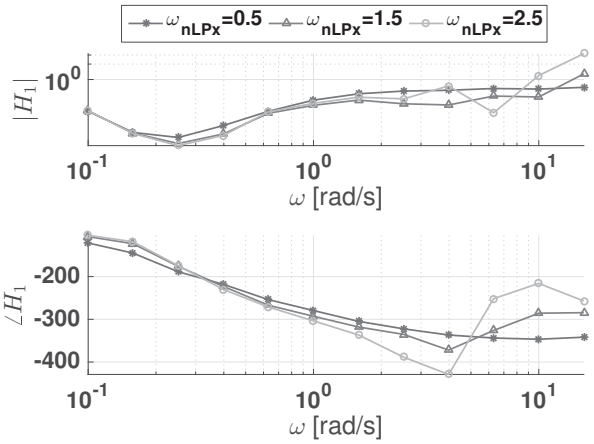

Fig. 13: Pitch frequency response function tailored to a Hover MTE.

in motion characteristics between the tilt coordination filter and the surge translational channel. However, for the tailored OMCTs, surge motion is cued *more* than in actual helicopter flight. From figure 12b it can be seen that the magnitude becomes larger than 1, for some frequencies. This effect is due to crosstalk from pitch to surge. Similarly to figure 6, in figure 14 the high-pass break frequency on the pitch channel was varied.

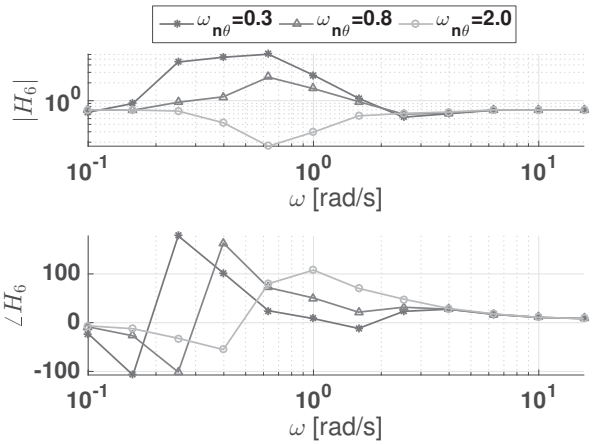

Fig. 14: Surge frequency response function tailored to a Hover MTE.

It can be seen that by tuning the classical washout algorithm such that little coupling is expected from pitch to surge, the surge frequency response function resembles the original OMCT.

- There is little difference between the frequency response function for heave for the original OMCT and a tailored OMCT. This is an indication that in the classical washout filter, heave is mostly uncoupled with other DOFs.

With this methodology, notable differences in the motion cueing characteristics were identified for the pitch and surge axes. Most importantly it was seen that coupling between pitch and surge are directly visible in the frequency response plots figure 12a and figure 12b, as an addition to frequency response functions from the original OMCT.

For actual pilot-in-the-loop simulation, the human controller will influence the control input of the model and therefore the characteristics of the helicopter motion. A limitation of the preceding analysis is therefore that the amplitude and relative phase of different degrees of freedom are not only influenced by the dynamics and Mission Task Element, but also by pilot control behavior.

VALIDATION EXPERIMENT

Identified differences in the prediction of motion characteristics between a tailored OMCT and the current OMCT were validated with a pilot-in-the-loop experiment. The primary objective of this experiment is to study the influence of pilot control behavior on a tailored OMCT. Secondly, it interesting to see if upswing on the surge axis due to pitch-surge coupling has any influence of pilot fidelity ratings. Figure 15 shows a schematic representation of the experimental set-up.

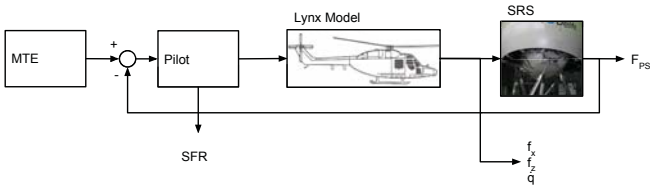

Fig. 15: Schematic flowchart of a pilot-in-the-loop simulation.

Experimental Set-up

For the validation experiment, the SIMONA Research Simulator (SRS) at Delft University of Technology, figure 16, was used. The SRS is a 6 Degree-Of-Freedom simulator developed for human-machine interface and handling qualities research. The motion system is hydraulic, consisting of 6 actuators. Figure 16 shows the exterior and the interior of the SRS.

(a) Exterior. **(b) Interior.**

Fig. 16: SIMONA Research Simulation (SRS).

The SRS is equipped with an 180 by 40 [*deg*] field of view collimated outside visual display, which together with a high quality scene detail and an update rate of 120 Hz results in high fidelity visual cues provided to the pilot. The visual cues are synchronized with the motion cues to within 10 [ms].

Control was provided to the pilot by means of a collective and a the longitudinal cyclic only. A basic 6 instrument set-up was provided digitally on the center Multi-Function Display (MFD) of the SRS

For this experiment, a non-linear 3-DOF mathematical model equal to that of the off-line analysis was implemented in the simulation architecture of SRS.

Mission Task Elements Similarly to the off-line analysis two MTEs were flown. Firstly a take-off and abort task was performed. Table 3 depicts desired and accurate performance according to Ref. 14 for this task. Dedicated visual cues for this task were implemented in the SRS visual display and are illustrated by figure 17.

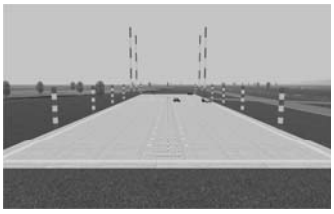

Fig. 17: Front view of the take-off and abort symbology.

Secondly a hover MTE was performed. Table 4 depicts desired and accurate performance according to Ref. 14 for this task. Figure 18a and figure 18b show dedicated visual cues implemented in the SRS visual display.

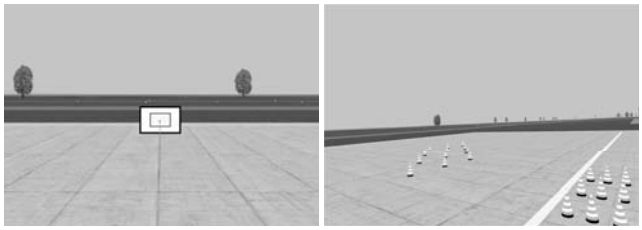

(a) Front. **(b) Diagonal.**

Fig. 18: View of the hover symbology.

Motion Cueing Settings Besides the MTEs, a second independent variable for this experiment was considered. In the off-line simulation, the most notable difference in motion characteristics between the tailored OMCT and the current OMCT was the upswing on the surge frequency response. This upswing was due to crosstalk from pitch to surge, influenced mostly by the high-pass break frequency on the pitch channel. It is therefore interesting to see the influence of this parameter on pilot fidelity ratings. To this end, four different motion cueing conditions were presented to the pilot. The high-pass pitch break frequency was varied, $\omega_{n_\theta} = 0.5$, 0.8, 1.2 and $1.5[rad/s]$. Other parameters were set similarly to the off-line simulation, given in table 2.

Experimental Procedure Three experienced helicopter pilots participated in this experiment. Credentials are presented in figure 5.

Table 5: Participants.

No.	Flight Hours	Type	Last Flight	Pilot Type
1	1000	CH47D-F	active	Military
2	1000	CH47D-F	active	Military
3	Over 4000	Alouette III, Cougar	2014	Military

Pilots were instructed to fly the simulator with a similar control strategy as they would fly the aircraft. They were also requested specifically to strive for desired performance as much as possible. After a familiarization period in which pilots were presented with all test conditions and were allowed to practice until a stable performance for both tasks was achieved, 8 test conditions were presented to the participant. Each test condition was flown until 3 consecutive runs with a stable performance were achieved. Thereafter the participant was asked to award a fidelity metric for that particular condition. To avoid any additional learning between runs, different motion settings were varied between conditions according to table 6.

Table 6: Test matrix for three participants.

Condition	Task	ω_{n_θ} s1	ω_{n_θ} s2	ω_{n_θ} s3
1	Hover	0.5	1.2	0.8
2	Hover	1.2	0.8	1.5
3	Hover	0.8	1.5	1.2
4	Hover	1.5	0.5	0.5
5	TO-A	1.2	1.2	1.5
6	TO-A	0.5	1.5	0.8
7	TO-A	1.5	0.8	0.5
8	TO-A	0.8	0.5	1.2

The motion output of the flight model was recorded. With these time-traces, tailored OMCTs were conducted. Secondly, the fidelity of the different motion settings of the classical washout algorithm will be assessed using the Simulation Fidelity Rating (SFR) scale, given in appendix B, as was proposed by Perfect and Timson in Ref. 18. The SFR assumes a high fidelity simulation when the attainable performance of the simulation is similar to the performance in the real helicopter with minimal task strategy adaptation. Although numerical values for the mathematical model were taken from a Lynx reference helicopter, model fidelity permits a direct comparison between simulator and helicopter performance. Performance will therefore be judged based on the experience of the participants.

Hypotheses

Since the model outcome is influenced by pilot control behaviour, it is expected that tailored OMCTs based on the experimental data will show differences with the off-line analysis. Moreover, since pilots will not fly every run with a similar performance, it is expected that the experimental data will show variance on both the gain and phase of the OMCT predictions.

A secondary purpose of this experiment is to validate the pitch-surge coupling subjectively by means of the SFR scale. Since upswing is present in the frequency response function for surge at low values of ω_{n_θ}, it is expected that the pilot with rate these simulations will a higher SFR, indicating a lower total fidelity of the simulation. It is hypothesized that participants will rate the simulation with a lower SFR for higher values of ω_{n_θ}, indicating a higher total fidelity of the simulation.

RESULTS

Objective Metrics - Time Domain

The performance of both MTEs is presented in figure 19 and figure 20 respectively, in terms of longitudinal position and altitude. Also visualized are desired and adequate performance according to Ref. 14.

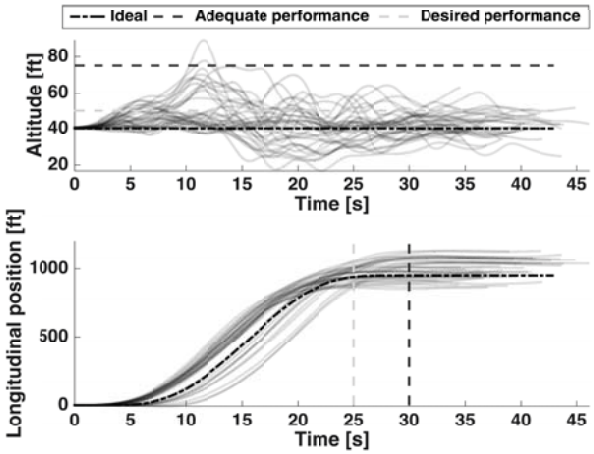

Fig. 19: Altitude and longitudinal position for the Take-Off and Abort MTE.

From figure 19 it can be seen that the take-off and abort maneuver was performed with adequate performance. However, during the experiment it was noticed that participants had trouble identifying the endpoint of the maneuver. This resulted in an overshoot or undershoot of the desired end location of the task. As was identified by Atencio in 1993, Ref. 19, due to a limited field-of-view, lateral and longitudinal drift is known problem for rotorcraft simulations.

Figure 20 shows the performance for the hover task. It can be seen that for most runs adequate performance was achieved. However, also for this task, difficulty to maintain longitudinal position was identified. Furthermore it can be seen that for the first participant the initial altitude of the maneuver was set too high, at 20 [ft]. This was corrected for the subsequent participants. This was considered acceptable, since the participant corrected the altitude within 5 [s].

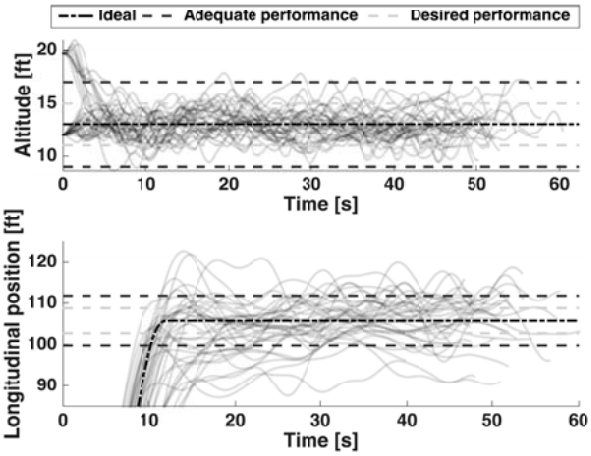

Fig. 20: Altitude and longitudinal position for the hover MTE.

Objective Metrics - Tailored Input Signals

The time traces of specific forces and rotational accelerations from the experiment were converted to the frequency domain and the relative phases were computed, according to the methodology proposed in the off-line analysis. Figure 21 and figure 22 show the amplitude and relative phase for the take-off and abort and hover task, respectively.

The following observations were made.

- The highest amplitude for the pitch input signals is around 1$[rad/s]$.
- For surge input signals, the amplitude is higher for low frequencies than the off-line analysis, for the take-off and abort task. Furthermore, it can be seen that a large variance is present in the relative phase for low frequencies for the hover task.
- The amplitude in heave is larger as compared to the off-line analysis. The controller is better capable to keep the aircraft at a constant altitude than a human operator. The relative phase for both tasks does not show a clear trend, not unlike the off-line analysis.

Objective Metrics - Tailored OMCT

A tailored OMCT was computed by using a tailored set of input signal for each test run. Result will be displayed here using a parameter set given in table 2. figure 24a and figure 23a show the pitch frequency response functions for the tailored OMCTs, together with the off-line analysis and the original OMCT. The mean and standard deviation in the form of an error bar are shown for all participants and all test conditions.

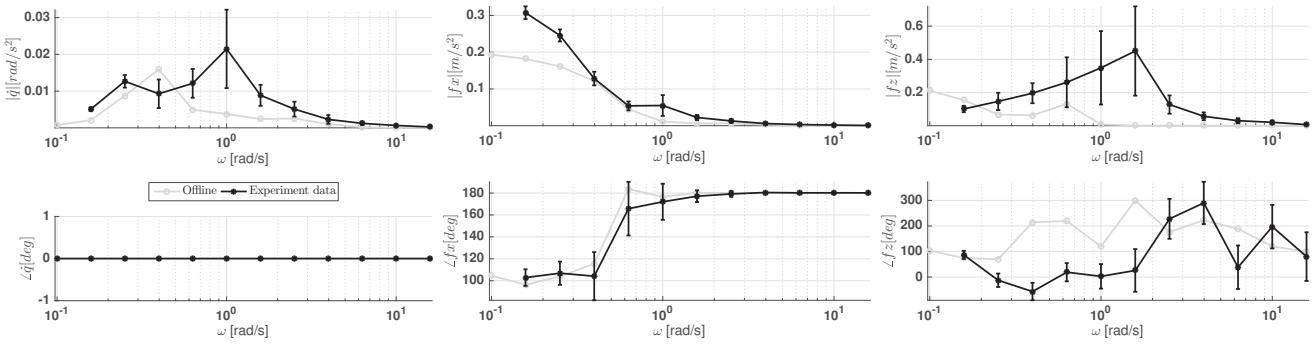

(a) Pitch. **(b) Surge.** **(c) Heave.**

Fig. 21: Amplitude and phase spectrum for a tailored OMCT based on experimental data for a take-off and abort MTE.

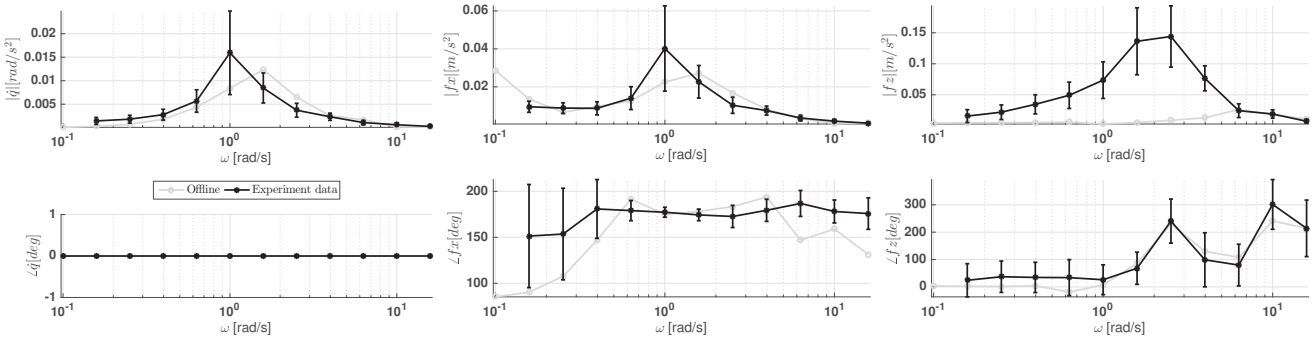

(a) Pitch. **(b) Surge.** **(c) Heave.**

Fig. 22: Amplitude and phase spectrum for a tailored OMCT based on experimental data for a hover MTE.

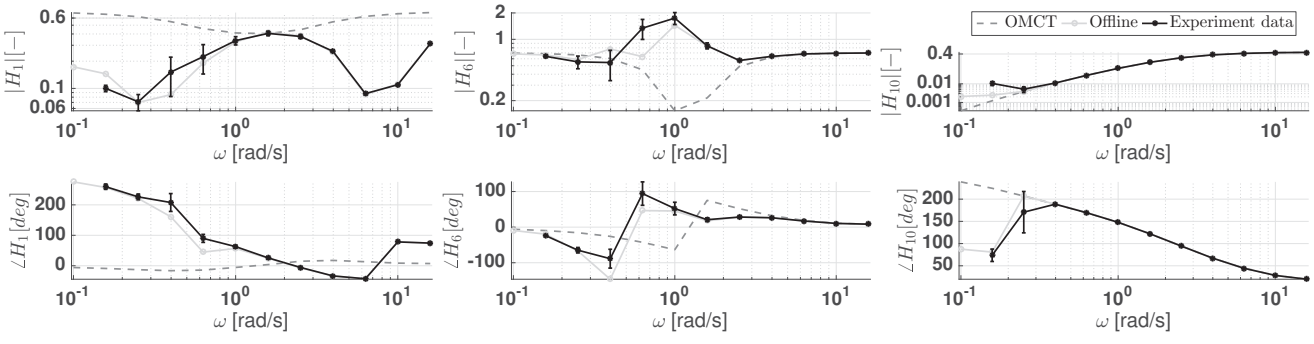

(a) Pitch. **(b) Surge.** **(c) Heave.**

Fig. 23: Frequency response functions for the take-off and abort MTE.

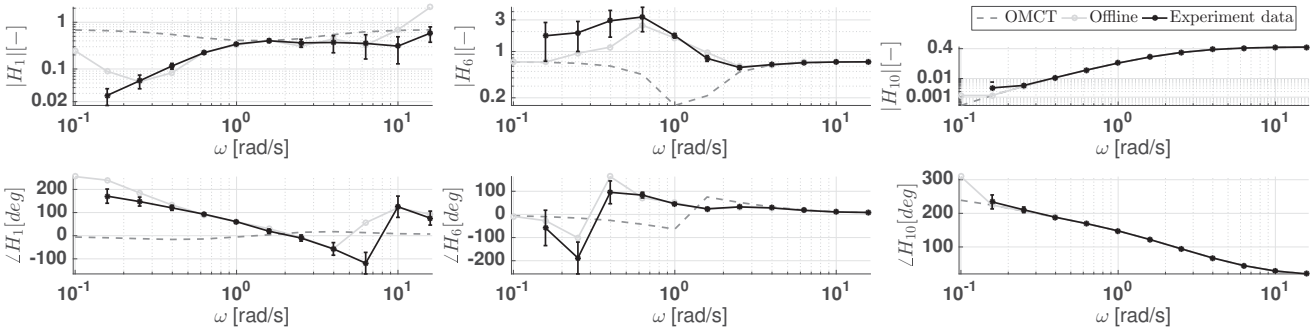

(a) Pitch. **(b) Surge.** **(c) Heave.**

Fig. 24: Frequency response functions for the hover MTE.

From figure 24a it can be seen that the experimental data follows the same trend as the off-line analysis. It can be seen that no data point exists for the lowest OMCT frequency point, $\omega = 0.1[rad/s]$. This is because the tasks do not provide sufficient measuring time for the lower frequencies of the OMCT. Furthermore there is variance on the amplitude and phase for frequencies below 0.3 and above 2 $[rad/s]$ for the hover MTE. This is an indication that a combination of pilot input and turbulence has an effect on the motion characteristics. Variance above 2 $[rad/s]$ is thought to originate from turbulence, since no variation is present in the take-off and abort task. Furthermore there is a large variance present at lower frequencies of the take-off and abort MTE, according to figure 23a.

Figure 24b and figure 23b show the surge frequency response function for the tailored OMCT. Again, experimental data is compared to the original OMCT and the off-line analysis. It can be seen that for the hover MTE, upswing on the surge axis at low frequencies is higher for the experimental data as compared to the off-line analysis. Furthermore, it can be seen that there is large variance at the low frequency response points. Secondly it can be seen that for the take-off and abort task indicated upswing is also present. However, variance exists on frequency point 0.4, 0.6 and 1.0 $[rad/s]$ of the OMCT.

Finally, figure 24c and figure 23c show the heave frequency response function for the tailored OMCT, for both MTEs. It can be seen that there is little difference between a tailored OMCT and the original OMCT, both for the off-line simulation and the experimental data. However at low frequencies, both the off-line and the experimental data predict a higher amplitude than the original OMCT.

Crosstalk from Pitch to Surge For the secondary objective of this experiment a tailored OMCT was performed for every test run on the motion cueing settings of that particular test run. Figure 25 shows the mean of the surge frequency response functions for the 4 different motion conditions, for the hover task. It can be seen that a similar trend is visible as was seen during the off-line analysis, presented in figure 14. For low values of the high-pass break frequency on the pitch channel, there is an upswing in the surge specific force at low frequencies.

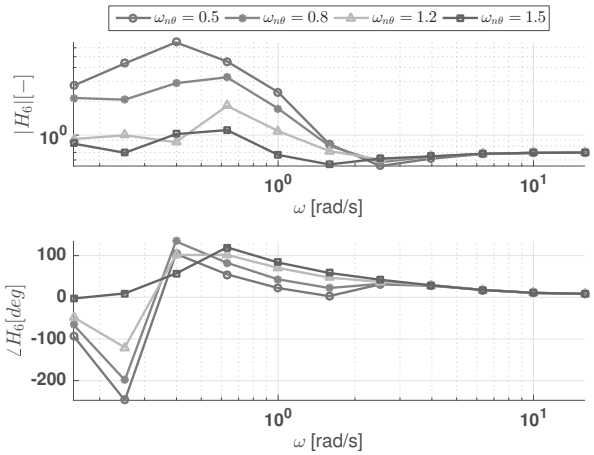

Fig. 25: Frequency response function for surge motion characteristics for 4 motion conditions, hover.

A similar result was obtained from the take-off and abort MTE, presented in figure 26, where the surge frequency response functions for the take-off and abort task are presented.

Subjective Metrics - SFR

Pilot ratings have been summarized for the different test conditions in figure 27. Similar motion conditions are rated with a different SFR, but in some cases also with a different fidelity level. It can be seen that condition 2 is awarded the lowest fidelity ratings for the hover MTE. For the take-off and abort MTE, condition 3 seems of the lowest fidelity. From discussion about the ratings during the experiment, participants gave the following explanations.

- Participant 1 rated all conditions equally, with an SFR of 2, indicating all simulations were of fidelity level 1. As explanation he gave: *"we are trained to not trust the motion of the helicopter, but rely on instruments as much as possible"*.
- Participant 2 indicated for the second test condition in hover: *"turbulence interfered with motion"*. Further-

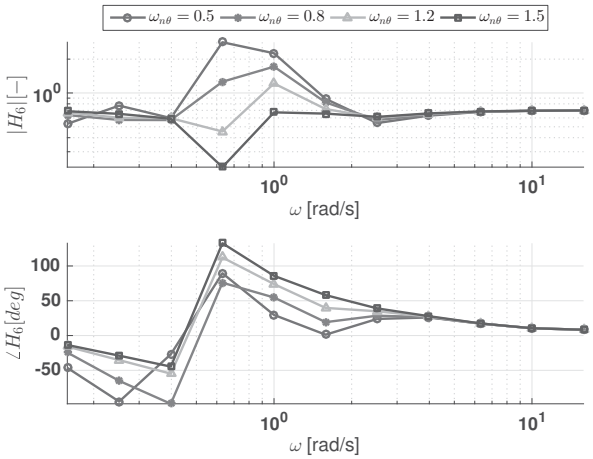

Fig. 26: Frequency response function for surge motion characteristics for 4 motion conditions, take-off and abort.

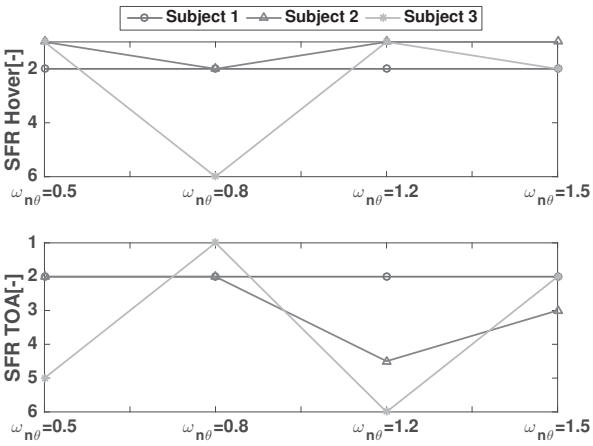

Fig. 27: Awarded SFR rating per test condition for both the Hover and Take-off and Abort MTEs.

more, he indicated for the third test condition in the take-off and abort task *"I miss the motion cue for longitudinal acceleration"* and *"for this condition I relied more on my instruments."*

- Participant 3 indicated for the second test condition in hover: *"There is a delay in the response of the aircraft"*. Secondly, he indicated for the first test condition in the take-off and abort task: *"There was little difference in motion, but due to large travel in de cyclic stick, the simulation was less realistic."* Lastly he indicated for the third test condition in take-off and abort: *"The pitch movement for this condition was too large for my liking."*

DISCUSSION

In this paper the extent to which the current OMCT is representative for rotorcraft was studied. The effect of assumptions in the input signals on the frequency response functions was studied. It should be noted however, that this analysis is limited to the classical washout algorithm. Furthermore any effects of the cueing hardware on the frequency response functions were not taken into account.

A methodology was proposed to compute a set of input signals that potentially better represents motion of a specific helicopter model and two specific MTEs. This was done by modeling the amplitude and relative phase for the three longitudinal axes. The following advantages have been identified. The first advantage is that crosstalk between the degrees of freedom is now directly visible as an addition to the direct frequency response functions. This makes it possible to see the effect of a parameter in the classical washout algorithm on all axes simultaneously. For tuning purposes, the off-axis performance can therefore be assessed directly. For example, the influence of the high-pass break frequency on the surge axes directly be tested by varying $\omega_{n\theta}$ and computing the surge frequency response function, without the need for cross tests. Secondly, test duration is reduced significantly, since all response functions can be computed using only one sweep through the frequencies.

A downside of the proposed method is firstly that the tailored OMCT outcome is very sensitive to the signal-processing of the amplitude and relative phase spectra. Since there are often no exact estimates of the amplitude and phase form the FFT at the OMCT frequencies, a least-squares fit had to be made. It was seen that this fit is very sensitive to the degree and amount of splines used. Furthermore it was seen that the resulting signals often had an amplitude 50 times smaller than the current OMCT. This might give problems with the signal-to-noise ratio of sensors in practical implementation of such a test in the future. Thirdly the shape of the frequency response functions is less intuitively related to the classical washout algorithm.

Finally it should be noted that the model output is not only influenced by the dynamics of the helicopter, but also by the pilot control input. For any off-line analysis in the future, it might be considered to use a pilot model that better portrays pilot control behavior.

A validation experiment on the SRS was subsequently conducted. It was seen that pilot input did have a noticeable influence on the motion characteristics of the simulation, especially for surge and pitch. An explanation this can be sought in the fact that the relative phase of the surge input spectrum for both tasks varies largely depending on the run, as can be seen from figure 22b and figure 21b. Especially for hover, the relative phase varies between 100 and 200 $[deg]$. This in turn is due to the fact that the drag component in the specific force is unpredictable since it is influenced by pilot control input and due to turbulence present in the hover task. If the relative phase is close to 200 $[deg]$, specific force due to the pitch rotation will be canceled out by acceleration in surge direction of the helicopter body. The amplitude for the pitch frequency response plot will thus be lower. If the relative phase is close to 100 $[deg]$, surge due to pitch rotation will be canceled out less. The amplitude for the OMCT pitch frequency response function will higher.

Performing the analysis with a more complex mathematical model might influence the relative phase between pitch and surge and will therefore also influence the fidelity of a

tailored OMCT. It would therefore be interesting to see the influence of a horizontal tail, the presence of a spring and/or drag forces on the main rotor on the relative phase between pitch and surge.

Finally a subjective analysis of four motion cueing settings was performed to see if pilot subjective opinion was is agreement with the objective metrics. No trend was found in accordance with the hypothesis that a low high pass pitch break frequency would results in a better SFR rating. An explanation can be sought in two aspects of the simulation.

- Firstly the model fidelity might have interfered with the SFR evaluation. Pilots indicated that they frequently encountered a pilot-induced-oscillation, especially in the training phase. This was due to the fact no augmentation was present in the model and pilots had to close the pitch feedback loop manually. Secondly pilots commented on the stick travel as being too large as compared to real helicopter flight. During the experiment, pilot were instructed to focus on the motion fidelity as much as possible. However, in one case the pilot reported still giving a bad fidelity metric, due to unusually large stick travel.
- Secondly performance was judged subjectively by the pilot and the experiment leader. There was implemented a display which plotted the velocity and altitude profile of the run real-time. However, the ADS-33 criteria were not included in this graph.

CONCLUSION

The objectives of this paper were (1) to investigate the extent to which the OMCT is representative for rotorcraft in the longitudinal plane, (2) to investigate whether a potentially superior set of input signals better representing helicopter motion can be defined and (3) to validate potential differences in the prediction of motion characteristics between an OMCT based on the helicopter motion and the current OMCT with a pilot-in-the-loop experiment.

The following conclusions can be drawn.

1. The current OMCT is representative for heave motion characteristics, but issues arise when looking at the pitch and surge motion characteristics. Firstly surge-pitch coupling is represented incorrectly in the direct pitch frequency response function. Secondly the results from the tests for pitch-surge and surge-pitch coupling are hard to interpret. Finally there is a large sensitivity to rate limiting in the tilt coordination channel.
2. Notable differences in the motion cueing characteristics were identified for the pitch and surge axes, when tailoring a set of input signals to a specific helicopter model and two Mission Task Elements.
3. From the validation experiment it was firstly concluded that, although pilot control behavior significantly affects pitch and surge motion characteristics according to a tailored OMCT, the main trend of the frequency response functions was determined by the dynamics of the helicopter model. Secondly it was concluded that the observed changes in motion characteristics due to different cueing settings were not accompanied by a reported loss of motion fidelity by the pilots.

RECOMMENDATION

The ultimate objective of an objective motion cueing evaluation is to find a set of input signals that incorporates all important characteristics of helicopter motion, such that it can be used to evaluate a variety of different simulators and tasks. To this end, it is recommended to evaluate the current set of input signals of the OMCT for a variety of models, also incorporating lateral motion, and mission task elements using a similar method presented in this article. Furthermore it is recommended to implement a pilot model in future off-line analysis, such that sensitivity of the OMCT to the pilot task strategy is mitigated.

An Objective Motion Cueing Test with input signals more closely resembling helicopter motion will enable simulator engineers to evaluate the motion cueing fidelity in a more representative way. This in turn could support the development and configuration of motion cueing algorithms, which are more suitable for the task at hand: the training of helicopter pilots.

Author contact: Wouter Dalmeijer,
W.H.Dalmeijer@student.tudelft.nl;
Ivan Miletović, I.Miletovic@tudelft.nl;
Olaf Stroosma, O.Stroosma@tudelft.nl;
Marilena Pavel, M.D.Pavel@tudelft.nl.

APPENDIX A

The non-linear, longitudinal equations of motion used for this research were:

$$\dot{u} = -g\sin\theta_f - \frac{D}{m}\cos(\theta_f) + \frac{T}{m}\sin(\theta_{1c} - a_1) - qw \quad (5a)$$

$$\dot{w} = g\cos\theta_f - \frac{D}{m}\sin(\theta_f) - \frac{T}{m}\cos(\theta_{1c} - a_1) + qu \quad (5b)$$

$$\dot{q} = -\frac{Th_R}{I_{yy}}\sin(\theta_{1c} - a_1) \quad (5c)$$

$$\dot{\theta}_f = q \quad (5d)$$

Here $\dot{u}$ and $\dot{w}$ are the derivatives of the body velocities and $\dot{q}$ is the pitch rotational acceleration. Furthermore θ_f is the pitch angle of the helicopter, θ_{1c} is the longitudinal cyclic input and α_1 is the longitudinal flapping angle.

Drag D is computed only taking into account the drag of the fuselage. Thrust T is given by $T = C_T \frac{1}{2}\rho V^2 S$, where C_T is computed by means of iterative solving for the inflow velocity of the main rotor, λ_i, using the the Blade Element Method and Glauert, given here:.

$$CT_{BEM} = \frac{1}{4}a_0\sigma\left(\frac{2}{3}\theta_0(1 + \frac{3}{2}\mu^2) - (\lambda_c + \lambda_i)\right) \quad (6a)$$

$$CT_{GLA} = 2\lambda_i\sqrt{\left(\frac{V}{\Omega R}\cos(\alpha_c - a_1)\right)^2 + \left(\frac{V}{\Omega R}\sin(\alpha_c - a_1) + \lambda_i\right)^2} \quad (6b)$$

In these expressions, a_0 is lift coefficient of a rotor blade, σ is the rotor solidity, θ_0 is the collective input, Ω is the rotational velocity of the main rotor and R the rotor radius. The longitudinal flapping coefficient a_1 was computed from:

$$a_1 = \frac{\frac{8}{3}\mu\theta_0 - 2\mu(\lambda_c + \lambda_i) - \frac{16}{\gamma}\frac{q}{\Omega}}{1 - \frac{1}{2}\mu^2} \tag{7}$$

Here the airspeed V, the angle of attack of the control plane α_c, the non-dimensional aircraft velocity μ and the inflow velocity of the main rotor due to the aircraft velocity λ_c were computed according to the following set of equations.

$$V = \sqrt{u^2 + w^2} \tag{8a}$$

$$\alpha_c = \theta_{1c} - \tan^{-1}\frac{w}{u} \tag{8b}$$

$$\mu = V\frac{\cos\alpha_c}{\Omega R} \tag{8c}$$

$$\lambda_c = V\frac{\sin\alpha_c}{\Omega R} \tag{8d}$$

APPENDIX B

REFERENCES

1 Anon, "Attachment F. Frequency-domain Motion Cueing System Performance Test," *Doc 9625, Manual of Criteria for the Qualification of Flight Simulators*, Vol. I - Aeropl, ICAO, third edition, 2009.

2 Hosman, R. J. A. W., Advani, S. K., and Takats, J., "Status of the ICAO Objective Motion Cueing Test," Flight Simulation Research, New Frontiers, Conference Proceedings, 2012.

3 Advani, S. K. and Hosman, R. J. A. W., "Revising Civil Simulator Standards - An Opportunity for Technological Pull," Proceedings of the Modeling and Simulation Technologies Conference, 2006.
doi: 10.2514/6.2006-6248

4 Sinacori, J. B., "The Determination of Some Requirements for a Helicopter Flight Research Simulation Facility," Technical report, NASA Ames Research Center, Moffet Field, CA, 1977.

5 Advani, S. K., Hosman, R. J. A. W., and Potter, M., "Objective Motion Fidelity Qualification in Flight Training Simulators," Proceedings of the Modeling and Simulation Technologies Conference, 2007.
doi: 10.2514/6.2007-6802

6 Hosman, R. J. A. W. and Advani, S. K., "Are Criteria for Motion Cueing and Time Delays Possible ? Part 2 . Manual of Criteria for the Qualification and Testing of Flight Simulation Training," Proceedings of the Modeling and Simulation Technologies Conference, 2013.

7 Hosman, R. J. A. W. and Advani, S. K., "Design and Evaluation of the Objective Motion Cueing Test and Criterion," *The Aeronautical Journal*, Vol. 120, (1227), 2016, pp. 873–891.

8 Stroosma, O., "Applying the Objective Motion Cueing Test to a Classical Washout Algorithm," Proceedings of the Modeling and Simulation Technologies Conference, 2013.
doi: 10.2514/6.2013-4834

9 Seehof, C., Durak, U., and Duda, H., "Objective Motion Cueing Test - Experiences of a New User," Proceedings of the Modeling and Simulation Technologies Conference, 2014.
doi: 10.2514/6.2014-2205

10 Reid, L. D. and Nahon, M. A., "Flight Simulation Motion-base Drive Algorithimns: Part 1-Developing and Testing the Equations," Technical Report 296, UTIAS, Toronto, 1985.

11 Meiry, R. L., "The Vestibular System and Human Dynamic Space Orientation," Technical report, Massachusetts Institute of Technology, Man-Vehicle Lab, Boston, MA, 1966.

12 Hodge, S. J. and White, M. D., "Challenges in Roll-Sway Motion Cueing Fidelity : A View from Academia," Royal Aeronautical Society Flight Simulation Group Conference on "Challenges in Flight Simulation", 2015.

13 Wiskemann, C. M., Drop, F. M., Pool, D. M., van Paassen, M. M., Mulder, M., and Bülthoff, H. H., "Subjective and Objective Metrics for the Evaluation of Motion Cueing Fidelity for a Roll-Lateral Reposition Maneuver," Proceedings of the 70th American Helicopter Society International Annual Forum, 2014.

14 Anon, *ADS-33E-PRF, Aeronautical Design Standard Performance Specification Handling Qualities Requirements for Military Rotorcraft*, United States Army, Redstone Arsenal, Alabama, 2000.

15 Padfield, G. D., *Helicopter Flight Dynamics : The Theory and Application of Flying Qualities and Simulation Modeling.*, John Wiley & Sons., Washington, DC, 2007.

16 Bramwell, A. S. R., "Rotor forces and choice of axes," *Bramwell's Helicopter Dynamics*, edited by G. Done and D. Balmford, Butterworth-Heinemann, second edition, 2001, pp. 26–28.

17 Hoblit, F. M., *Gust Loads on Aircraft: Concepts and Applications*, AIAA, Washington, DC, 1988, pp. 42–44.

18 Perfect, P., White, M. D., Padfield, G. D., Erdos, R., and Gubbels, A. W., "A Rating Scale for the Subjective Assessment of Simulation Fidelity," *The Aeronautical Journal*, Vol. 118, (1206), 2014, pp. 953–974.

19 Atencio, A. J., "Fidelity Assessment of a UH-60A Simulation on the NASA Ames Vertical Motion Simulator," Technical report, NASA Ames Research Center, Moffet Field, CA, 1993.

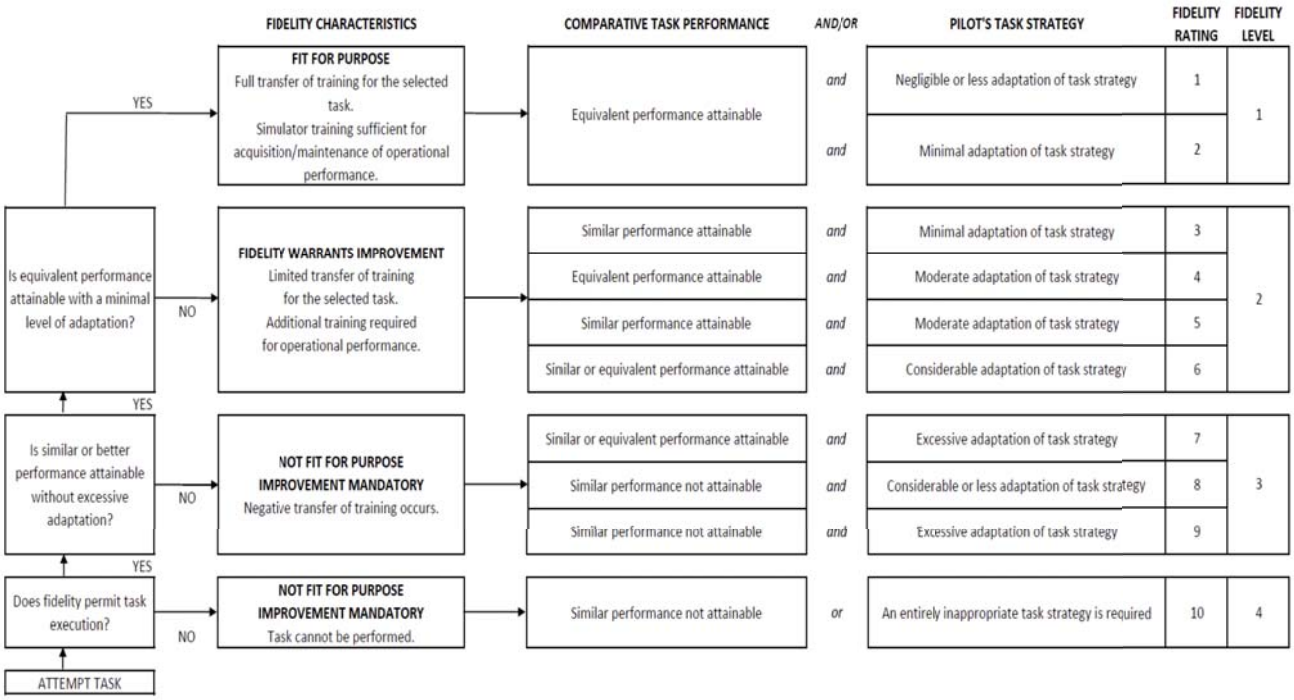

Fig. 28: Simulation Fidelity Rating scale, used for subjective evaluation of motion fidelity, taken from Ref. 20.

20 Beard, S. D., Reardon, S. E., Tobias, E. L., and Aponso, B. L., "Simulation System Fidelity Assessment at the Vertical Motion Simulator," Proceedings of the 69th American Helicopter Society International Annual Forum, 2013.